


Digital image correlation strain measurement of ultra-high-performance concrete-prisms under static and cyclic bending-tensile stress

Stefan Harenberg¹  | Matthias Pahn¹ | Viktória Malárics-Pfaff² | Frank Dehn² | Antonio Caggiano³ | Diego S. Schicchi³ | Sha Yang³ | Eddie Koenders³

¹Fachgebiet Massivbau und Baukonstruktion, Technische Universität Kaiserslautern, Kaiserslautern, Germany

²Institut für Massivbau und Baustofftechnologie, Karlsruher Institut für Technologie, Karlsruhe, Germany

³Institut für Werkstoffe im Bauwesen, Technische Universität Darmstadt, Darmstadt, Germany

Correspondence

Stefan Harenberg, Fachgebiet Massivbau und Baukonstruktion, Technische Universität Kaiserslautern, Paul-Ehrlich-Straße, D-67663 Kaiserslautern, Germany.
Email: stefan.harenberg@bauing.uni-kl.de

Abstract

This paper provides experimental results on investigations for the validation of photogrammetric strain measurements of ultra-high-performance concrete (UHPC)-prisms subjected to static and cyclic bending-tensile stress. For this purpose, 4 static and 5 cyclic test series were performed. Damage progresses during loading are monitored by means of a digital image correlation (DIC) system and a clip gauge. The control of the DIC by trigger lists and the measurement noise as a function of the measurement rate are examined. All static tests were performed force controlled with the same testing speed and the same measuring rate of DIC and clip gauge. All cyclic tests were performed with the same upper and lower stress levels but with different loading rates. During the static tests, the DIC can be used to make accurate strain measurements before UHPC failure. In the cyclic tests, the measurement noise of the DIC decreases with an increasing measuring rate. The tests performed confirm the control of the DIC by trigger lists for cyclic tests on UHPC-prisms and show that the measurement noise is negligible in static and cyclic tests.

KEYWORDS

cyclic bending tests, DIC, fatigue, photogrammetry, UHPC

1 | INTRODUCTION

Ultra-high-performance concrete (UHPC) is a composite material characterized by a greater strength and higher durability than a conventional concrete. On the one hand, UHPC is characterized by a low permeability to carbon dioxide, moisture migrations, chloride attacks, and sulfate ingresses. These higher durability skills permit to design longer service

life structures with subsequent reduced maintenance costs.^{1,2} On the other hand, the high strength capacity allows to minimize the cross-sectional area of concrete structural frames of those modern buildings made of UHPC.¹ However, a main drawback of UHPC structures is represented by their increased slenderness and susceptibility to vibration.³ Consequently, fatigue behavior is a key issue worthy of investigation in this kind of buildings.⁴ This applies to structures such as wind turbines and high-speed-train bridges, which are exposed to bending-tensile stresses. However, existing research on fatigue of concrete is mainly concerned with normal and higher strength concrete under compressive

Discussion on this paper must be submitted within two months of the print publication. The discussion will then be published in print, along with the authors' closure, if any, approximately nine months after the print publication.

This is an open access article under the terms of the Creative Commons Attribution License, which permits use, distribution and reproduction in any medium, provided the original work is properly cited.

© 2019 The Authors. Structural Concrete published by John Wiley & Sons Ltd on behalf of International Federation for Structural Concrete

stress. Fatigue failure behavior depends on many parameters which mainly influence the number of load cycles needed to reach the total collapse of a structure.^{5,6}

Most of the available codes and current approaches analyze the concrete fatigue performance through empirical rules.⁷ They are based on the well-known Wöhler concepts⁸ (and the so-called S-N Basquin relationship) in which it is supposed that the fatigue damage is linearly accumulated (in a log-log law) with the number of cycles/reversals at a particular stress level.^{9,10} As example, it can be mentioned the smeared crack approach for concrete by¹¹ in which the S-N criterion is transformed into the damage description, taking into account the stress increment and the number of cycles per material point.¹² Although, these kind of approaches have been valuably used in practical applications, codes, and standards, they completely avoid deeper explanations of the mechanisms which drive the damage initiations and triggering of concrete-fatigue behavior.¹³

Plenty of experimental researches have been recently published in literature which deals with investigating the fatigue behavior of both normal concrete and UHPC. For example, tests performed in unreinforced,¹⁴ steel bar-reinforced,¹⁵ and fiber-reinforced¹⁶ UHPC have been recently investigated. Many of these works showed a huge scatter in terms of fatigue performances of the composite which can be actually attributed to the high variability of the composite material (in terms of strengths, stress levels, inner meso-structures, distribution of fibers/reinforcements, strain-hardening/softening mechanisms, and test specimen type and size) which hugely influence the fatigue response.^{17–27}

There is a lack of knowledge about the behavior of UHPC under cyclic bending-tensile loading. Outstanding test results on UHPC, which are worth of mentioning were published by *Brosge*²⁸ and *Kessler-Kramer*²⁹ while for tensile-tests by *Fitik*.²⁴ Therefore, within the scope of the DFG-Priority-Program 2020 “Cyclic Damage Processes in High Performance Concretes in the Experimental Virtual Lab”, the Department of Concrete Structures and Structural Engineering of the *TU Kaiserslautern*, the Institute of Construction and Building Materials of the *TU Darmstadt* and the Institute of Concrete Structures and Building Materials of the *Karlsruhe Institute of Technology (KIT)* are running a research project titled “Micromechanical behavior of high performance concrete under cyclic loading at various moisture and thermal conditions”. Aims of these activities are the experimental and the numerical investigations of the UHPC material degradation under cyclic tensile- and bending tensile-stress.

In this paper an experimental program is shown that deals with the measurement of the fatigue behavior of UHPC. The accuracy of static and cyclic strain measurements using photogrammetry as a function of the measuring rate is

investigated. This measuring method, also known as digital image correlation (DIC), enables noncontact measurement of deformations on the surface of structural elements by means of an applied pattern. Furthermore, the control of the DIC by so-called trigger lists is examined. The results of the DIC are compared with those of a clip gauge. This is used to measure the crack mouth opening displacement (CMOD) of a notched beam or prism. After this general introduction about the State-of-the-Art and motivations of this research, the paper is organized as follows. Section 2 reports the analyzed materials and methods. The experimental setup is described in Section 3. Then, Section 4 deals with the considered experimental program and the cyclic test protocols. After that, Section 5 discusses the experimental results and analyzes and compares the measurement methods used. Finally, some concluding remarks and future research lines are described in Section 6.

2 | MATERIALS AND SPECIMENS

The specimens were molded at the Laboratory of the Institute of Concrete Structures and Building Material of the KIT. A unique reference UHPC-mixture, provided and agreed through the central DFG-Priority-Program 2020, has been used for all the test-series. This mixture is characterized by a maximum aggregate size of 0.5 mm and a water-cement ratio of 0.24. Table 1 gives an overview of the mixture composition: microsilica, quartz flour, and powder were used as constituents. The UHPC mixture was prepared by using a pan mixer. Firstly, cement and microsilica were saturated and mixed; then the aggregate was added and mixed with the cement and microsilica. Subsequently, water and super-plasticizer were added. After molding, the specimens were sealed in the formwork for 24 hr, then stored under water for 7 days and matured afterwards in a laboratory climate at 20°C and 65% RH until testing.

Bending tests were carried out on unreinforced standard prisms measuring 40 × 40 × 160 mm³ (according to EN 196-1³⁰). The applicability of the classical beam theory for prisms with these dimensions was verified by a classical

TABLE 1 Concrete constituents of the UHPC “RU1”

Constituents	Mass (kg/m ³)
Cement CEM I 52,5 R	795.0
Microsilica	168.6
Quartz flour	198.4
Quartz sand	971.0
Water	187.9
Super-plasticizer	24.1

Abbreviation: UHPC, ultra-high-performance concrete.

linear-elastic FEM calculation with the program RFEM5 in.³¹ In order to compare the measurement results of the DIC with a clip gauge, a notch with a depth of 6.7 mm and a width of 3 mm was milled starting from the bottom surface of the specimens in accordance with EN 14651³² (Figure 1). At the time of the tests, the specimens reached between 50 and 54 days of maturations. According to the dimensions of the specimens (Figure 1), the material tests were also performed on prisms according to EN 196-1.³⁰ They provided a compressive strength of 107 N/mm² and a bending tensile strength of 11.3 N/mm².

3 | EXPERIMENTAL SETUP

Aim of the experimental program is the validation of the strain measurement of UHPC-prisms, subjected to cyclic bending-tensile stress, by means of DIC. Analogous to investigations by *Khor et al.*,³⁵ a classical measurement method is used for comparison purpose against the results registered with the DIC. Preliminary tests have shown that almost identical results to DIC cannot be achieved with strain gauges and linear variable displacement transducer.³⁶ Therefore a clip gauge of type UB-5A from Tokyo Measuring Instruments Lab was attached under the notch to compare the measured CMOD with the DIC-results (Figure 2). This clip gauge has a measuring range between 3 and 8 mm and a measurement accuracy of $1,000 \times 10^6$ strain/mm.

The ARAMIS 5 M industrial DIC-system is used and based on two cameras with a monochrome CCD chip with $2,448 \times 2050$ pixels. With the electronic shutter, exposure times of 0.1 ms–2 s, adjustable and continuous frame rates of up to 15 fps (frames per second) are possible. With a strain accuracy of 0.01%, the strain measurement range is 0.02% to >100%. With measuring volumes from 10×8 mm up to $5,000 \times 4,150$ mm, 2D and 3D displacements as well as strains can be measured on the front of the specimens surface. The system also allows the measurement of out-of-plane displacements as the two cameras require a calibration of angle and distance between the cameras and the region of interest. For this purpose, the captured pictures are divided into subsets. All subsets must have a different, random pattern, which is achieved by spraying a black and white

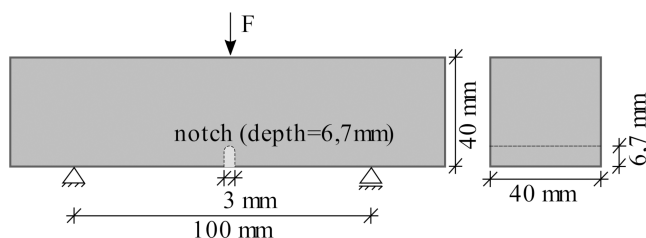


FIGURE 1 Specimen geometry

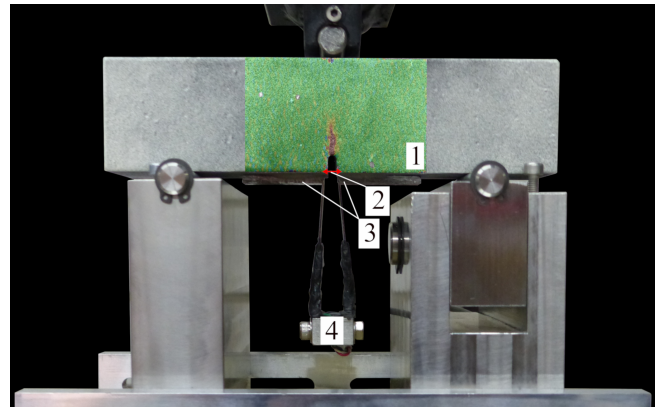


FIGURE 2 Experimental setup: 1 = DIC pattern, 2 = DIC-extensometer, 3 = glued on metal plates to attach the clip gauge, 4 = clip gauge. DIC, digital image correlation

pattern onto the specimen's surface.³⁷ Initially, the specimen surface is inspected for roughness and, if necessary, sanded smooth. Afterwards, a standard white acrylic paint is sprayed on in two to three layers. Then, a black speckle pattern is applied with graphite spray. The required fineness of this pattern was examined in preliminary tests (Figure 3). It has been shown that only with a fine pattern (Figure 3—right) a sufficient measuring accuracy can be achieved. This pattern is applied at a distance of 15 cm by moving the spray head quickly over the specimen. The density of the black color dots depends on the speed of the movement of the spray head and should correspond to Figure 3—right pattern.

The tests were performed in a two-column frame from Instron with a servo-hydraulic cylinder that can apply a maximum static and cyclic force of 10 kN. Preliminary tests have shown that the upper and lower stress levels can only be reliably applied up to a loading rate of 3 Hz. The entire experimental setup is shown in Figure 4.

4 | EXPERIMENTAL PROGRAM

The experimental tests were carried out at the Laboratory of the Department of Concrete Structures and Structural Engineering of the TU Kaiserslautern. Particularly, to perform fatigue tests, the lower stress-level S_{\min} and the upper one



FIGURE 3 Variation of the speckle pattern (left: Coarse, right: Fine)

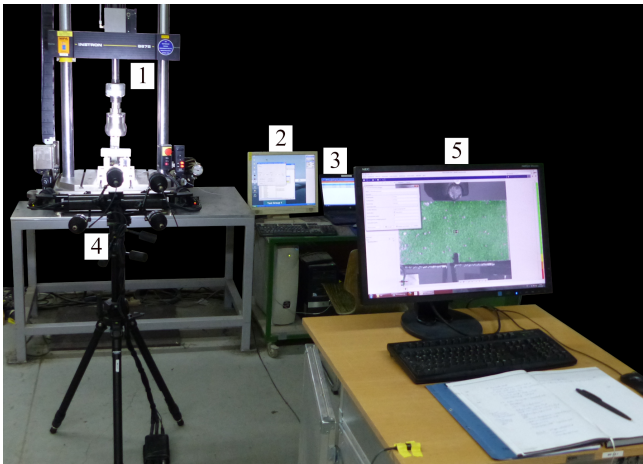


FIGURE 4 Experimental setup: 1 + 2 = testing machine, 3 = PC for the clip gauge, 4 = DIC, 5 = control of the DIC. DIC, digital image correlation

S_{\max} must be defined. Therefore, the experimental program is divided into static and cyclic test series. All specimens of a test series originate from the same formwork and all specimens of the experimental program are made of the same UHPC batch.

In order to avoid any kind of influence deriving from different casting and production times, the test series for static and dynamic tests were systematically differentiated and marked according to the casting sequence (Table 2).

The static tests were performed load-controlled on four different test series (n° VS1, VS2, VS3, and VS4). In accordance to EN 12390-5³³ the testing speed was set as 0.06 MPa/s. During the tests the displacements of the specimen was measured with the DIC and for comparison purpose with a clip gauge. The DIC was controlled by a preset measuring rate of 15 fps (frames per second). To determine

the behavior of the UHPC after cracking, the CMOD of the clip gauge was recorded at a measuring rate of 1.2 kHz.

The cyclic tests were performed load-controlled on five different test series (n° VC1, VC2, VC3, VC4, and VC5) with the same lower- and upper stress-level but different loading rates as specified in Table 2. This procedure was chosen because the measurement noise of the DIC depends on the measuring rate, which has to be selected according to the loading rate.³⁴ Measurement noise is a fluctuation of the results underlying any measurement system and defines the accuracy of the system. If this is larger than the measuring range, the measurement method is unsuitable.

In preliminary tests it was determined that the strain amplitude of UHPC-prisms under cyclic bending-tensile loading cannot be measured completely with a preset measuring rate-controlled DIC.³⁶ Therefore the DIC was controlled by the force signal of the machine via trigger lists. In further tests, specimens with an upper stress level of, for example, $S_{\max} = 60\%$ shall be cyclically loaded. The number of load cycles until failure can be several million. For reasons of test duration, a minimum loading rate of 0.5 Hz was therefore selected. The maximum loading rate was selected according to the machine (see Section 3). The loading rate of 2 Hz was chosen because the preliminary tests were carried out with it.³⁶ The other loading rates were chosen with a focus on higher loading rates. In order to take pictures with the DIC via the trigger lists at the minimum and maximum load, the fade time of the camera must be four times the loading rate. The fade time corresponds to the measuring rate of the DIC. Preliminary tests have shown that the system does not take pictures with a lower fade time. In four cyclic test series an image of the specimens surface is taken as soon the applied load corresponds to S_{\min} and S_{\max} . In the test series VC3 an additional image was taken between S_{\min}

TABLE 2 Experimental program

Test series	Formwork number	Specimen number	Loading	S_{\max} (%)	S_{\min} (%)	Loading rate (Hz)	Loading speed (MPa/s)	DIC rate (Hz)	CG rate (Hz)
VS1	5	3 (A,B,C)	Static	-	-	-	0.06	15	1,200
VS2	11	3 (A,B,C)	Static	-	-	-	0.06	15	1,200
VC1	7	3 (A,B,C)	Cyclic	90	10	0.5	-	2	50
VC2	9	3 (A,B,C)	Cyclic	90	10	2.0	-	8	50
VS3	14	3 (A,B,C)	Static	-	-	-	0.06	15	1,200
VC3	13	3 (A,B,C)	Cyclic	90	10	2.5	-	10	50
VS4	18	3 (A,B,C)	Static	-	-	-	0.06	15	1,200
VC4	15	3 (A,B,C)	Cyclic	90	10	2.75	-	11	50
VC5	17	3 (A,B,C)	Cyclic	90	10	3.0	-	12	50

Abbreviations: CG, clip gauge; DIC, digital image correlation.

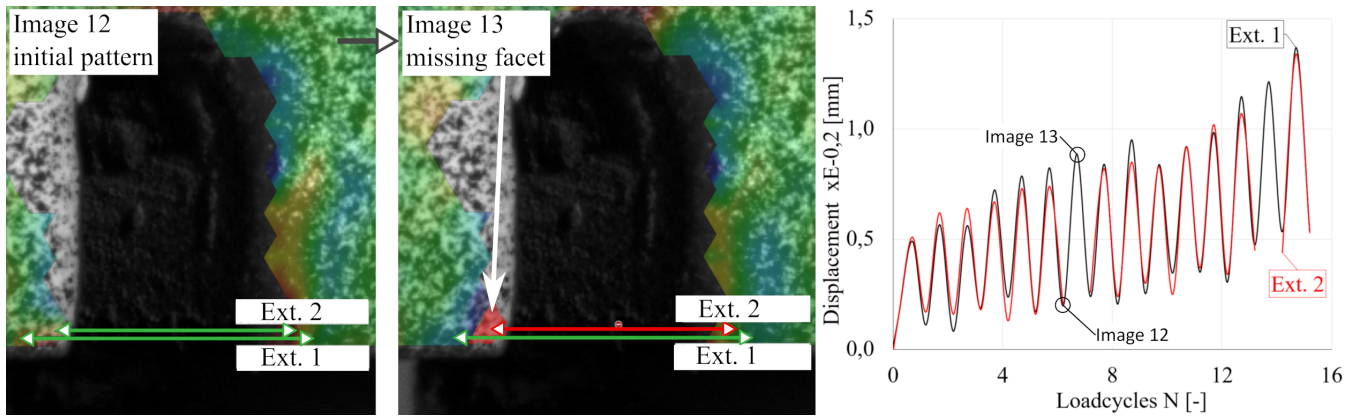


FIGURE 5 Failure of digital image correlation facet in a cyclic test

and S_{\max} . During the cyclic tests the CMOD was recorded with the clip gauge at a measuring rate of 50 Hz.

5 | RESULTS AND DISCUSSION

With the clip gauge a displacement Δ_C between two points is measured that has to be converted into a strain ε_C with a reference length L . To enable a comparison with the DIC-results, two measuring points were placed on the DIC-pattern next to the notch edge and to the specimens edge. Between this measuring points a virtual extensometer was placed (Figure 2). The measurement results were also output as displacements Δ_D . The difficulty of the evaluation is to select suitable measuring points on the DIC pattern because the clip gauge measures 5 mm below the specimen due to the supports (Figure 2). Taking into account the failure of some DIC-pattern facets in some images, the DIC extensometer was placed as possible to the lower edge of the specimen (Figure 5). As with the clip gauge, the DIC-extensometer cannot be placed exactly to the edge of the notch. This is negligible, since the comparison of two DIC-extensometers shows that no strains occur in this area (see Ext.1/Ext. 2—Figure 5). Small differences results from the measurement noise. Therefore, the strain ε_C and ε_D are calculated with the notch width of 3 mm as the reference length L .

Due to the different distance to the neutral axis of the specimen, the DIC-extensometer and the clip gauge will measure different displacements under a deflection δ (Figure 6). This difference can be calculated in a simplified way depending on the deflection δ and taking into account the vertical distance Δ_M between the Clip Gauge and DIC measurement points:

$$\Delta_C - \Delta_D = \Delta_{C-D} = \left(\frac{\delta}{\sqrt{l^2 + \delta^2}} \right) \cdot \Delta_M \quad (1)$$

For comparison the strains are calculated with the modified displacement Δ_C as follows:

$$\varepsilon_D = \frac{\Delta_D}{L} \quad \varepsilon_C = \frac{(\Delta_C - \Delta_{C-D})}{L} \quad (2)$$

5.1 | Static tests

Figure 7 shows the results of the static tests. The results of each test series are shown separately and the graphs are marked according to the experimental program (Table 2). The ending CG represents the clip gauge and the ending DIC the digital image correlation. No DIC results are shown for the specimen VS1A, as the measurements cannot be evaluated due to a memory error. Since there is no stress in the measuring area at the notch, the machine force is plotted to the y-axis.

The measured strain of the clip gauge and the DIC are close together for each specimen in each test series. More-

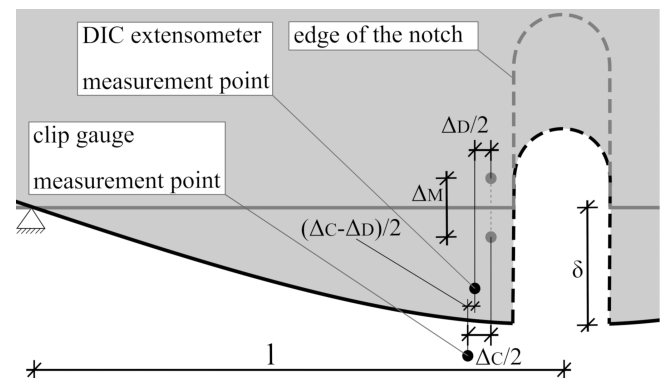
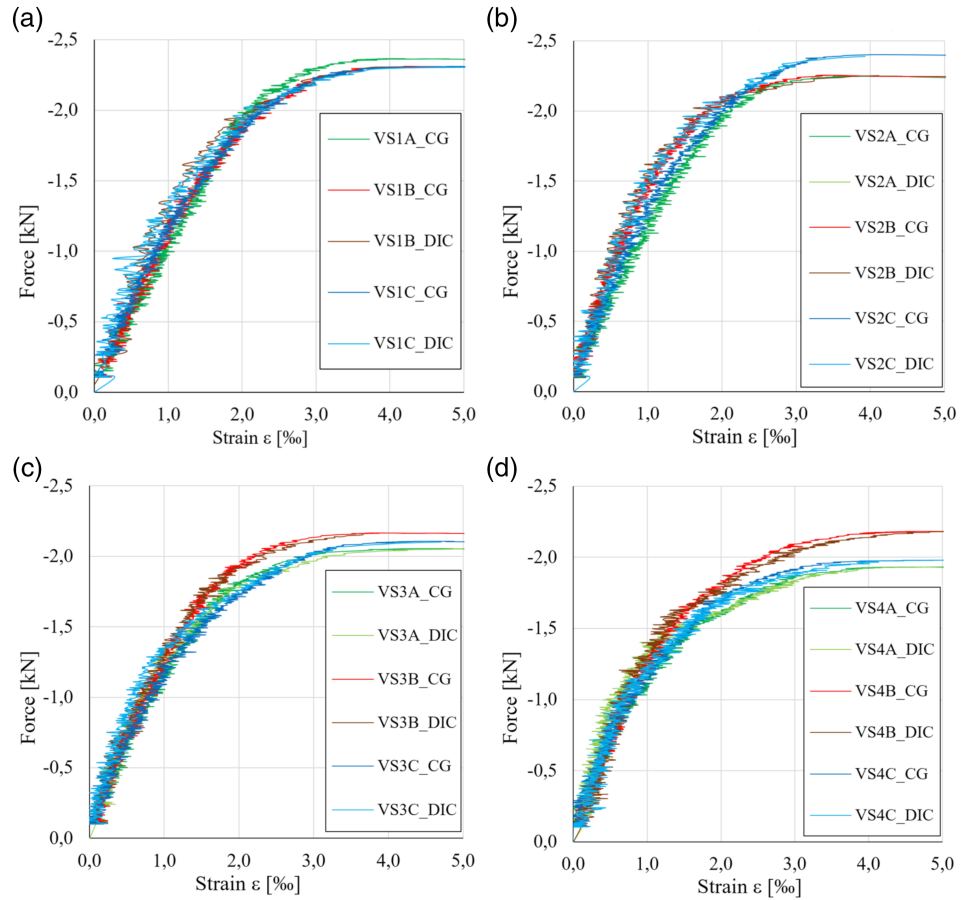


FIGURE 6 Measuring difference between digital image correlation and clip gauge due to deflection Δ

FIGURE 7 Force-strain-curves of the static test-series



over the strain of all specimens in each test series also matches well. Also with regard to the linear course up to a force of 1 to 1.25 kN and a fracture strain between 4 and 5 ‰, the results are in good agreement between the test series. In addition, the measurement accuracy must also be taken into account for the comparison of both measurement methods. The accuracy of DIC measurements is described by the *SD* of the measured values.³⁴ This is calculated by the deviation Δ_ϵ of the measured values from the mean value curve (Figure 8). This deviation is equal to the measurement noise (see Section 4). Figure 9 shows the *SDs* of the clip gauge and the DIC for each specimen with a mean value curve. As can be seen, the variance of the CG *SD* is clearly larger compared to the DIC in the test series VS1. The reverse situation can be seen for the test series VS2 and VS4 and it is largely identical for the test series VS3. The mean value curves of both measurement systems do not show a uniform course. It must be considered that the respective measuring rates of the clip gauge and the DIC remained the same in all test series (Table 2). Combined with the variance of the *SDs*, the results permit the conclusion that the accuracy of the CG and the DIC are on the same level for static tests. However, due to the slower measuring rate of the DIC of 15 Hz and the sudden failure of the unreinforced UHPC, the material behavior after the occurrence of a macro crack

cannot be recorded, compared to the clip gauge. If this is not required, the DIC is recommended as measurement method due to the easier application. Furthermore, in contrast to the clip gauge, no notch is required for the DIC.

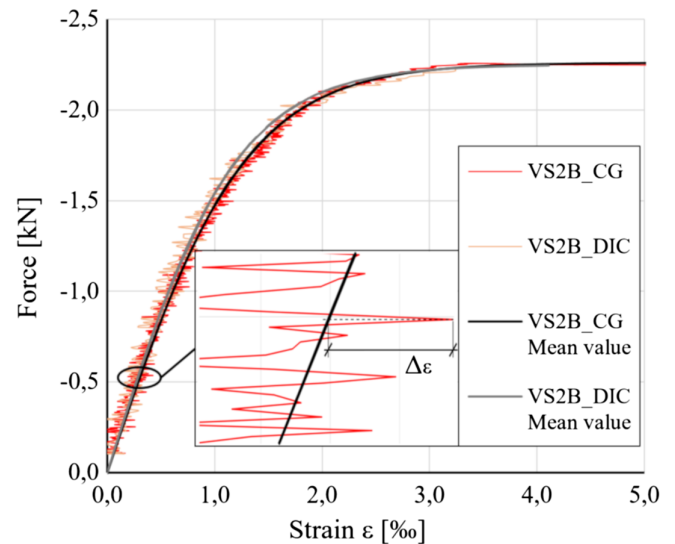


FIGURE 8 Deviation $\Delta\epsilon$ of the measured values from the mean value curve—SPEC. VS2B

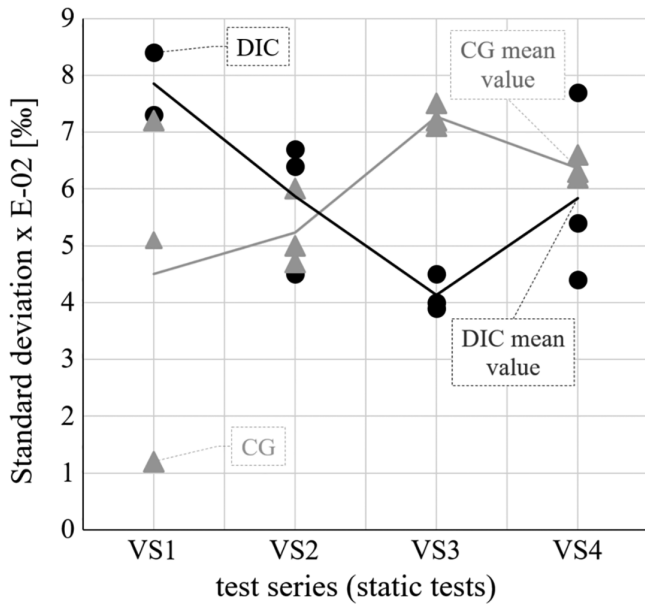


FIGURE 9 *SD* of the clip gauge and the digital image correlation for static tests

5.2 | Cyclic tests

Figure 10 shows the results of the cyclic tests. The strain due to cyclic loading is plotted over the load cycles N . For better clarity, only selected results of each test series, which are marked according to the experimental program, are plotted separately. The ending CG indicates the clip gauge and the ending DIC the digital image correlation. In the test series VC1, no continuous measurement with the DIC was possible due to the slow load frequency of 0.5 Hz. Therefore no comparison between DIC and clip gauge is possible. It shows that the control of the DIC by trigger lists is only possible at a higher loading rate. The measurement data of the first load cycles are missing for all DIC-measurements. This is due to the DIC, whose measurement procedure via trigger lists can only be started after the testing machine has started. Otherwise no images are taken, analogous to test series VC1.

The measured strain of the CG and the DIC are close together for each specimen in the test series VC2, VC4, and VC5. In test series VC3, where an additional image was taken per load cycle N , the strain amplitude of the DIC is lower than that of the clip gauge. It is assumed, that due to the images taken between S_{\min} and S_{\max} , the exposure time of the cameras were too weak, which means that the measured deformations are smaller than they actually are. This effect could be avoided by a stronger exposure but than the very fine pattern on the specimens surface will be overexposed.

In all test series the strain increases greater with decreasing number of load cycles N and the fracture strain between

4 and 5.5 % corresponds to the static tests (Figure 10a-d). Moreover the curves of the increasing strain correspond to the usual 3-phase fatigue behavior of UHPC after crack initiation. This complies with the usual fatigue behavior of UHPC and excludes a general measurement failure. Not shown graphs of the respective tests (VC2C, VC3B/C, VC4B, and VC5B/C) correspond in their qualitative course to the graphs shown in Figure 10. They also have a typical 3-phase fatigue curve. The increase of the second phase after crack initiation is also flatter with increasing number of load cycles N and the fracture strain is in the same range. An applied load without initial crack initiation was not achieved in any test.

The *SDs* of the CG and DIC measurements are shown in Figure 11 as a function of the DIC measuring rate. The CG-measuring rate was 50 Hz in each test series and is plotted for comparison. Analogous to the static tests, the determination is carried out by the deviation Δ_ε (Figure 8) of the measured values from the mean value curves ε_{\max} and ε_{\min} . The results show, that the *SD* of the DIC decreases with an increasing measuring rate. In general, the *SD* of the CG is 0.04 % lower than the DIC. For the measuring rates 10, 11, and 12 Hz, the variance of the CG *SD* is about 0.006 % less than the DIC. As the results in Figure 10 show, this deviation is negligible due to the magnitude of the measured strains. The similarity of the results between the CG and DIC as well as the slightly higher DIC *SD* of the measured values, confirm the control of the DIC by trigger lists for the strain measurement of UHPC-prisms under cyclic bending-tensile loading. However, the DIC must be controlled by trigger lists for complete recording of the strain amplitude of the specimen per load cycle. As the results of the tests series VC3 show, only images of S_{\min} and S_{\max} shall be taken.

6 | CONCLUSIONS

This paper reports on an experimental study to validate the strain measurement of the degradation of UHPC-prisms under cyclic bending-tensile stress by DIC. For this purpose, the measurement noise of the DIC and a clip gauge was determined and compared in alternating static and cyclic tests. The experimental program includes 4 static and 5 cyclic test series.

In the static tests the course of the load-strain curves and the *SD* of the measured values were considered. In all tests, the load-strain curves of both measuring methods match well and the *SD* is at a similar level in all tests. A comparison of the test results of all specimens also shows good agreement as well as a fracture strain between 4 and 5 %. However the agreement of the results of both measuring methods is only achieved before a macrocrack occurs. With the DIC, no material behavior after the occurrence of a macro crack can

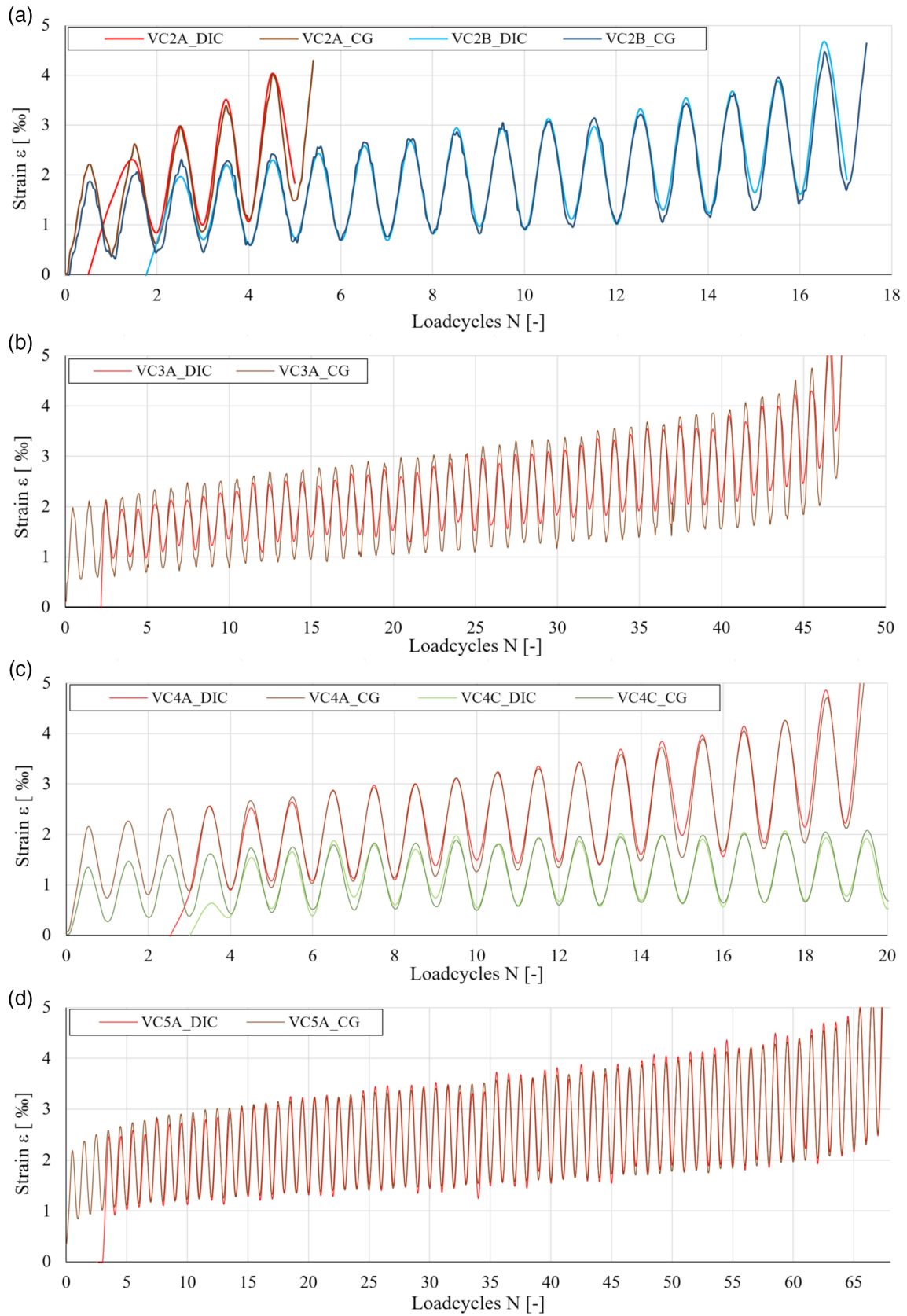


FIGURE 10 Increasing strain due to cyclic loading of the cyclic experiments

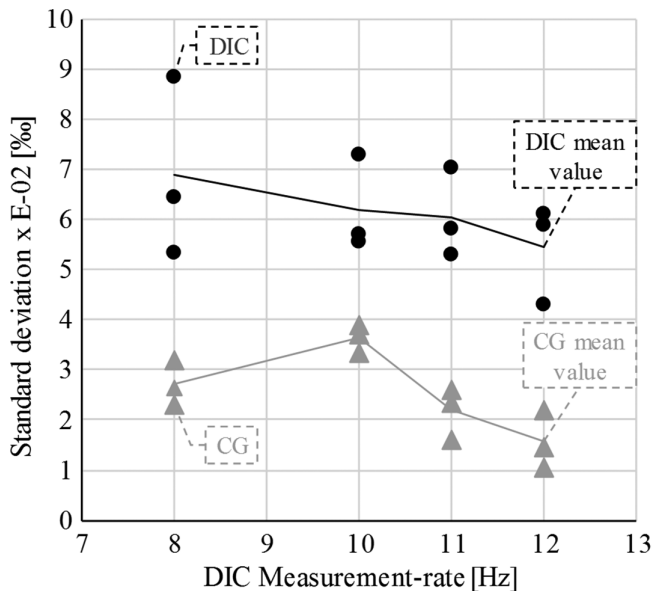


FIGURE 11 SD of the clip gauge and the digital image correlation for cyclic tests (clip gauge measurement rate = 50 Hz)

be recorded. Therefore the application of the clip gauge is only recommended if the recording of the material behavior after the occurrence of a macro crack is required. If the DIC is used, the loading speed must allow a sufficiently accurate recording, taking into account the maximum measuring rate.

In the cyclic tests the measurement noise of the DIC and a clip gauge was determined at five different loading rates. The DIC was controlled by trigger lists via the force signal of the machine. As the results of the first tests series VC1 show, a loading rate larger than 0.5 Hz has to be selected for this purpose. Otherwise no images will be recorded with the DIC. Furthermore, the results of the tests series VC3 show that only images at S_{\max} and S_{\min} should be taken with the DIC. Otherwise the strains will not be measured completely. The results of the test series VC2, VC4, and VC5, where only images were recorded at S_{\max} and S_{\min} , show a good agreement of the DIC measurements with the clip gauge measurements. The measurement noise of the DIC is slightly larger, which is negligible with regard to the value of the measured strains. This measurement noise decreases with increasing loading rate. In conclusion, the cyclic tests confirm the strain measurement with the DIC using trigger lists. Based on the results, the DIC is recommended for measuring rates between 8 and 12 Hz to investigate the fatigue behavior of UHPC specimens. This measurement range is relatively small and can be extended to 15 Hz with the existing DIC system if another testing machine is used (see Section 3). For this measuring rate the measurement noise have to be investigated again in further tests. Newer DIC systems enable higher measurement rates, which could further extend the measurement rate.

The advantage of the DIC is the ease of application and the strain measurement of an increasing crack over the component height as well as over a significantly larger width, due to a pattern with any number of measurement points (Figure 2). In addition, due to the missing notch, the DIC can be used to check and visualize possible stress redistributions during cyclic and static loading.

ORCID

Stefan Harenberg  <https://orcid.org/0000-0001-8294-415X>

REFERENCES

1. Wang D, Shi C, Wu Z, Xiao J, Huang Z, Fang Z. A review on ultra high performance concrete: Part II. Hydration, microstructure and properties. *Construct Build Mater.* 2015;96:368–377.
2. van der Haar C, Marx S. Development of stiffness and ultrasonic pulse velocity of fatigue loaded concrete. *Struct Concr.* 2016;2016(4):630–636.
3. Shi C, Wu Z, Xiao J, Wang D, Huang Z, Fang Z. A review on ultra high performance concrete: Part I. Raw materials and mixture design. *Construct Build Mater.* 2015;101:741–751.
4. Fehling E, Schmidt M, Walraven J, Leutbecher T, Fröhlich S. *Ultra-high performance concrete UHPC: Fundamentals, design, examples.* Berlin, Germany: John Wiley & Sons, 2014; p. 1–188.
5. Marx, S, Grünberg, J, Hansen, M, Schneider, M. *Grenzzustände der Ermüdung von dynamisch hoch beanspruchten Tragwerken aus Beton, Deutscher Ausschuss für Stahlbeton e.V. –DafStb-, Berlin, 2017, Band 618; 2017.*
6. Mallet GP. *Fatigue of reinforced concrete, state of the art review.* 2nd ed. London, England: Transport & Road Research Laboratory, HMSO; 1991.
7. Skar A, Poulsen PN, Olesen JF. A simple model for fatigue crack growth in concrete applied to a hinge beam model. *Engineering Fracture Mechanics.* 2017;181:38–51.
8. Wöhler A. Über die Festigkeitsversuche mit Eisen und Stahl. *Zeitschrift für Bauwesen.* 1870;XX:73–106.
9. Oh BH. Fatigue analysis of plain concrete in flexure. *J Struct Eng.* 1986;112(2):273–288.
10. Hordijk DA, Reinhardt HW. Numerical and experimental investigation into the fatigue behavior of plain concrete. *Exp Mech.* 1993;33(4):278–285.
11. Dobromil P, Jan C, Radomir P. Material model for finite element modelling of fatigue crack growth in concrete. *Proc Eng.* 2010;2(1):203–212.
12. Banjara NK, Ramanjaneyulu K. Experimental investigations and numerical simulations on the flexural fatigue behavior of plain and fiber-reinforced concrete. *J Mater Civil Eng.* 2018;30(8):04018151.
13. Jadallah O, Bagni C, Askes H, Susmel L. Microstructural length scale parameters to model the high-cycle fatigue behaviour of notched plain concrete. *Int J Fatigue.* 2016;82:708–720.
14. Makita T, Brühwiler E. Tensile fatigue behaviour of ultra-high performance fibre reinforced concrete (UHPFRC). *Mater Struct.* 2014;47(3):475–491.

15. Makita T, Brühwiler E. Tensile fatigue behaviour of ultra-high performance fibre reinforced concrete combined with steel rebars (R-UHPFRC). *Int J Fatigue*. 2014;59:145–152.
16. Wille K, El-Tawil S, Naaman AE. Properties of strain hardening ultra high performance fiber reinforced concrete (UHP-FRC) under direct tensile loading. *Cem Concr Compos*. 2014;48:53–66.
17. Bornemann R, Faber S. UHPC with steel-and noncorroding high strength polymer fibres under static and cyclic loading. *Proceedings of the international symposium on ultra-high performance concrete*. Kassel, Germany: Kassel University, 2004; p. 673–681.
18. Guvensoy G, Kocaturk A, Yerlikaya M. Mechanical behaviour of high performance steel fibre-reinforced cementitious composites under cyclic loading condition. *Proceedings of the international symposium on UHPC*. Kassel, Germany: Kassel University, 2004; p. 649–660.
19. Lappa ES, Braam CR, Walraven JC. Static and fatigue bending tests of UHPC. *Proceedings of the international symposium on ultra-high performance concrete*. Kassel, Germany: Kassel University, 2004; p. 449–458.
20. Mu B, Shah SP. Fatigue behavior of concrete subjected to biaxial loading in the compression region. *Mater Struct*. 2005;38(3):289–298.
21. Lappa ES, Rene C, Walraven C. Flexural fatigue of high and ultra-high strength fiber reinforced concrete. *Proceedings of International RILEM Workshop on high performance fiber reinforced cementitious composites in structural applications*. Ann Arbor, MI: Delft University of Technology, 2006; p. 509–518.
22. Grünberg J, Lohaus L, Ertel C, Wefer M. Multi axial and fatigue behaviour of ultra-high performance concrete. *Proceedings of the 2nd international symposium on ultra-high performance concrete*. Kassel, Germany: Kassel University, 2008; p. 485–494.
23. Lohaus L, Ramge P. Robustness of UHPC—A new approach for mixture proportioning. *Proceedings of the second international symposium on ultra high performance concrete*. Kassel, Germany: Kassel University, 2008; p. 113–120.
24. Fitik, B. Ermüdungsverhalten von ultrahochfestem Beton (UHPC) bei zyklischen Beanspruchungen im Druck-Zug-Wechselbereich [doctoral dissertation]. Technische Universität München; 2012.
25. Lohaus L, Elsmeyer K. Fatigue behaviour of plain and fibre reinforced ultra-high performance concrete. *Proceedings of the 3rd international symposium on UHPC and nanotechnology for high performance construction materials*. Kassel, Germany: Kassel University, 2012; p. 631–637.
26. Abbas S, Nehdi ML, Saleem MA. Ultra-high performance concrete: Mechanical performance, durability, sustainability and implementation challenges. *Int J Concr Struct Mater*. 2016;10(3):271–295.
27. Afrouhsabet V, Biolzi L, Ozbakkaloglu T. High-performance fiber-reinforced concrete: A review. *J Mater Sci*. 2016;51(14):6517–6551.
28. Brosge, S. Beitrag zur Ermüdungsfestigkeit von hochfestem Beton; 2001.
29. Kessler-Kramer, C. Zugtragverhalten von Beton unter Ermüdungsbeanspruchung, Bauingenieur- und Vermessungswesen der Universität Fridericana zu Karlsruhe (TH); 2002.
30. EN 196-1. Methods of testing cement – Part 1: Determination of strength; 2005.
31. Schultz-Cornelius M, Pahn M. Investigations on the size effect of thin structural elements made of UHPC. *Proceedings of the 4th international symposium on ultra-high performance concrete and high performance construction materials*, Kassel University, Kassel, Germany, 9th–11th March 2016, Book of Abstracts S, 2016; p. 71–72.
32. EN 14651: 12-2007. Test method for metallic fibre concrete—Measuring the flexural tensile strength (limit or proportionality [LOP], residual).
33. DIN EN 12390-5: 09-17. Testing hardened concrete—Part 5: Flexural strength of test specimens.
34. Jesse, F, Kutzner, T. *Digitale Photogrammetrie in der Bautechnik*, Bautechnik, Volume 90, Heft 11; 2013.
35. Khor W, Moore PL, Pisarski HG, Haslett M, Brown CJ. Measurement and prediction of CTOD in austenitic stainless steel. *Fatigue Fract Eng Mater Struct*. 2016;39:1433–1442.
36. Harenberg S, Caggiano A, Koenig A, et al. Micromechanical behavior of UHPC under cyclic bending-tensile loading in consideration of the influence of the concrete edge zone. *Proc Appl Math Mech*. 2018; 18:1–4.
37. Reis M, Adorna M, Jirousek O, Jung A. Improving DIC accuracy in experimental setups. *Adv Eng Mater*. 2019;2019:1900092.

AUTHOR BIOGRAPHIES



Stefan Harenberg
 Fachgebiet Massivbau und
 Baukonstruktion
 Technische Universität Kaiserslautern
 Paul-Ehrlich-Straße
 D-67663 Kaiserslautern, Germany
 stefan.harenberg@bauing.uni-kl.de



Matthias Pahn
 Fachgebiet Massivbau und
 Baukonstruktion
 Technische Universität Kaiserslautern
 Paul-Ehrlich-Straße
 D-67663 Kaiserslautern, Germany
 matthias.pahn@bauing.uni-kl.de



Viktória Malárics-Pfaff
 Institut für Massivbau und
 Baustofftechnologie
 Karlsruher Institut für Technologie
 Gotthard-Franz-Straße
 D-76131 Karlsruhe, Germany
 viktoria.malarics-pfaff@partner.
 kit.edu



Frank Dehn
 Institut für Massivbau und
 Baustofftechnologie
 Karlsruher Institut für Technologie
 Gotthard-Franz-Straße
 D-76131 Karlsruhe, Germany
 frank.dehn@kit.edu



Antonio Caggiano
Institut für Werkstoffe im Bauwesen
Technische Universität Darmstadt
Franziska-Braun-Straße
D-64287 Darmstadt, Germany
caggiano@wib.tu-darmstadt.de



Diego S. Schicchi
Institut für Werkstoffe im Bauwesen
Technische Universität Darmstadt
Franziska-Braun-Straße
D-64287 Darmstadt, Germany



Sha Yang
Institut für Werkstoffe im Bauwesen
Technische Universität Darmstadt
Franziska-Braun-Straße
D-64287 Darmstadt, Germany
yang@wib.tu-darmstadt.de



Eddie Koenders
Institut für Werkstoffe im Bauwesen
Technische Universität Darmstadt
Franziska-Braun-Straße
D-64287 Darmstadt, Germany
koenders@wib.tu-darmstadt.de

How to cite this article: Harenberg S, Pahn M, Malárics-Pfaff V, et al. Digital image correlation strain measurement of ultra-high-performance concrete-prisms under static and cyclic bending-tensile stress. *Structural Concrete*. 2019;20: 1220–1230. <https://doi.org/10.1002/suco.201900033>